A Mathematical Model and Analysis of the Onset and Growth of Shear Bands

David G. Torkington

Abstract

Under extreme shearing loads at high strain rates, many materials undergo intense deformation that is localised to narrow regions called shear bands. The localisation of the shear means that the heating due to mechanical dissipation is in turn localised. As such, shear banding has been identified as a likely generator of hotspots, and indeed has been empirically observed to cause local heating within explosives. Thus, from a safety standpoint, it is of critical importance to understand this phenomenon. Attempts at modelling shear bands using numerical hydrocodes are typically confronted by mesh distortion caused by the extreme strain rates involved. This motivates the work of a forthcoming paper, material from which we present herein. This work develops an analytical model that contains the essential aspects of shear band formation and growth. It considers one-dimensional Couette flow of a shear-thinning fluid, with a piecewise-constant viscosity that is much lower in the low-viscosity regime (where the shear stress exceeds a known yield value) than in the high-viscosity (low-shear) one. This shear-thinning is taken to be a purely mechanical process, thereby enabling a decoupling of the mechanical and thermal problems. Two setups are considered: Prescribed increasing shear stress on one end of the one-dimensional segment, zero shear stress on the other, and zero stress (and flow) initially; and prescribed increasing velocity on one end, zero velocity on the other, and zero flow initially. The analytical work from the forthcoming paper examines, using formal asymptotic methods, how the low-viscosity layer, which we identify with a shear band, initially forms and expands out from the boundary where the flow is being driven, and does so for each of the two setups. Improvements on previous analytical work in the area are made by not presupposing the velocity field within the material, but instead by solving for it using the momentum and constitutive equations, and by using a rheology that is not perfectly plastic. In each setup, asymptotic expansions for the growth of a shear band as a function of time are obtained.

1 Background & Motivation

Safety precautions are of paramount importance in the handling of energetic materials—that is, materials with large stores of chemical energy, such as fuels, propellants, and high explosives. Mechanical insults that result from low-velocity impacts can cause local shear within the material. In turn, this shear can bring about local heating due to mechanical dissipation, posing the risk of accidental initiation of the energetic materials.

In extreme cases, many materials exhibit narrow bands of intense plastic deformation. Heating due to mechanical dissipation in these regions leads to localised thermal softening of the material, enhancing the shear flow. Hence, a positive feedback loop is established, leading to ever-increasing shear rates within ever-localised zones, resulting in intense heat build-up within narrow regions. These narrow zones of extremely high shear rates are termed shear bands. Since the deformation in a shear band is highly localised, so is the resultant heating due to mechanical dissipation, and so shear banding is regarded as a likely mechanism for hotspot generation in energetic materials.

Focusing on high explosives, evidence of localised shearing within an explosive sample has been observed in recovered unexploded samples. Photographic evidence of shear banding was obtained by Field et al., whose photographs demonstrate ignition occurring in a shear band within a PETN sample [1]. Other empirical work on shear localisation within explosives includes those of Boyle *et al.*, Chen *et al.*, Dienes, Frey, and Afanas'ev and Bobolev [2, 3, 4, 5, 6]. All of these highlight localised shear as a likely generator of hotspots, and so shear banding is a critical phenomenon to investigate from a safety standpoint.

However, attempts at modelling shear bands with numerical hydrocodes typically are met by issues, either because the extreme strain rates (and hence extreme spatial gradients) within a shear band lead to mesh distortion, or because the small spatial scale of a shear band cannot be resolved accurately.

Such issues have motivated the development of analytical models that, although idealised so as to keep the mathematics tractable, succeed in giving insights into the physical processes at work within deformed explosives. Curtis analysed the axial pinching of a cylinder of explosive between two parallel plates, imposing that the axial velocity be linear in the axial ordinate, and derived an expression for the local rate of heating due to mechanical dissipation [7]. Under adiabatic conditions, this expression was used to calculate the temperature rise due to dissipation, and simple Arrhenius kinetics were used to represent the self-heating by the chemical reaction. An analysis of the simple shear of a slab of explosive, making use of analogous assumptions, was also performed by Curtis [8]. These works were able to correctly predict the observed relative sensitivities of PETN and a HMX-based explosive, but did not attempt to model the onset and growth of shear bands.

The work of the forthcoming paper, material from which we present herein, develops an analytical model that contains the essential aspects of shear band formation and growth. To capture the localised thermal softening that triggers shear banding, while also decoupling the mechanics from the thermal problem, a shear-thinning rheology is used, wherein the material's effective viscosity is reduced significantly when a threshold shear stress value is reached. Within the model, regions in which the shear stress exceeds this threshold are identified as shear bands.

As in Curtis's work on simple shear, homogeneity and the translation invariance that simple shear affords result in a one-dimensional model. On the other hand, a limitation of Curtis's analyses is the presumption of a linear velocity field. Naturally, the velocity field still needs to be subject to the constitutive equations governing the material response, which in Curtis's works, are taken to be the Levy–Mises equations of perfect plastic flow. To allow for more generality, rather than assuming it *a priori*, this work determines the velocity field from the equations describing the local conservation of linear momentum and the shear-thinning rheology, along with suitable boundary conditions. Moreover, the shear-thinning rheology allows for stress states strictly larger than the threshold value, unlike the saturation of stress that is characteristic of perfect plasticity.

The next section summarises the methods used by the forthcoming paper to derive the model. For brevity, details of some of the more subtle steps are suppressed; these can be found by consulting the forthcoming work.

2 Mathematical Model

2.1 Model assumptions

A two-dimensional, homogeneous slab of energetic material of height L is assumed to undergo horizontally-directed simple shear—horizontal planes in the slab remain parallel and maintain a constant separation, while translating relative to each other. In particular, no vertical pinching of the material occurs. The assumption of simple shear and of homogeneity jointly imply translation invariance along the horizontal x-direction, making it sufficient to treat the vertical interval $(0, L)$ as the domain. The top surface, $y = L$, is sheared in the positive x-direction; while the base, $y = 0$, is clamped and stationary throughout. More precisely, the behaviour at $y = L$ and $y = 0$ is specified by two separate sets of boundary conditions, which will be outlined in Subsection 2.3. See Figure 1 for an illustration of the geometric setup.

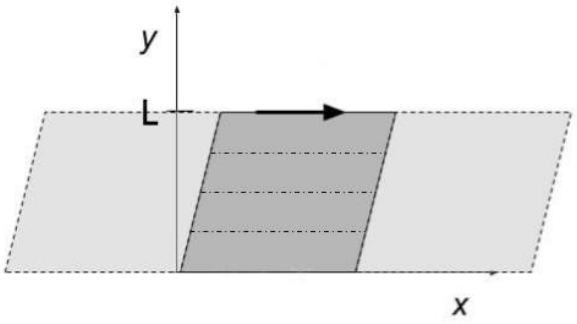

Figure 1: Simple shear of a slab of energetic material. Horizontal planes remain parallel and maintain a constant separation. Translation invariance in the x-direction means that it suffices to consider a representative vertical interval $(0, L)$. The top surface $y = L$ is sheared in the positive x-direction; while the base $y = 0$ is stationary throughout.

The shear stress $\tau(y,t)$ that is brought about by the simple shear is related to the horizontal velocity $u(y,t)$ of a material point y through the local conservation of linear momentum,

$$\frac{\partial \tau}{\partial y}(y,t) = \rho \frac{\partial u}{\partial t}(y,t), \tag{2.1}$$

where ρ denotes the mass density of the material, taken to be constant in space y and time t. To make (2.1) closed in one of $\tau(y,t)$ or $u(y,t)$, an additional datum relating $\tau(y,t)$ and $u(y,t)$ is required. This is provided by a constitutive equation describing the material's rheology.

2.2 Shear-thinning rheology

The goal of the forthcoming paper is to model shear bands, which, as outlined in Section 1, form in regions where the material has softened. Further, some notion of viscosity or internal friction must appear in the constitutive model to provide the possibility of local heating due to mechanical dissipation. Combining these two requirements motivate the shear-thinning, bi-viscous fluid rheology that is selected in this model. The behaviour of this rheology is illustrated in Figure 2.

For non-negative local shear rates $u_y(y,t)$, the constitutive equation for this rheology is

$$\tau(y,t) = \begin{cases} \eta u_y(y,t) & \text{if } \ 0 \leq u_y(y,t) < \gamma^*, \qquad (2.2) \\ \delta\eta u_y(y,t) + \eta\gamma^*(1-\delta) & \text{if } \ u_y(y,t) > \gamma^*. \qquad (2.3) \end{cases}$$

An analogous relation between $\tau(y,t)$ and $u_y(y,t)$ holds for negative local shear rates. By construction, the shear stress is continuous for $u_y = \gamma^*$ with a value of $\eta\gamma^*$. Each of the model parameters η, γ^* and δ is constant in space and time.

Remark. *Often, the partial derivative of a field f with respect to an independent variable v will be written as f_v:*

$$f_v \equiv \frac{\partial f}{\partial v}.$$

In words, the local shear stress $\tau(y,t)$ increases linearly for increasing local shear rate $u_y(y,t)$, with proportionality constant η, termed the unsoftened effective viscosity. When the shear rate reaches a threshold $\gamma^* > 0$ (when, by the above, $\tau(y,t) = \eta\gamma^*$), which is part of the rheological model and is material-specific, the material softens through a reduction in its effective viscosity from η to $\delta\eta$, for $0 < \delta \ll 1$. Beyond the threshold value, the shear stress continues to increase linearly for increasing shear rate, but with the

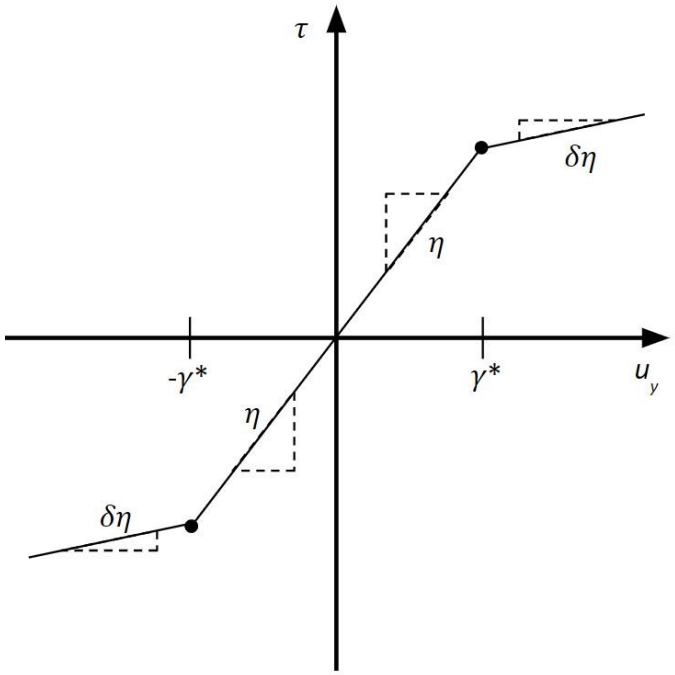

Figure 2: Graph of shear stress τ versus shear rate u_y for the shear-thinning rheology.

reduced proportionality constant $\delta\eta$. Regions where, at a certain time t, the local shear stress $\tau(y,t)$ is below the threshold $\eta\gamma^*$ will be termed hard; regions where the local shear stress exceeds $\eta\gamma^*$ are the shear bands of the mathematical model. The smallness of δ facilitates the formal asymptotic methods of Section 3, and physically corresponds to the extreme softness that is characteristic of materials that experience shear banding.

By definition, hard regions and shear bands will be separated by interface points where the local shear stress $\tau(y,t)$ exactly equals the threshold $\eta\gamma^*$. The trajectory of such interface points is *a priori* unknown, and so the field equations of the model must provide sufficient information for the trajectory to be calculated. Mathematically speaking, the field equations must describe a well-posed free boundary problem.

2.3 Field equations

As mentioned, two separate sets of boundary conditions are considered: prescribed shear stress at $y = 0$ and $y = L$, and prescribed velocity at these boundary points. In the latter case, if velocity as a function of time is given at $y = 0$ and $y = L$, then acceleration as a function of time is also known here. Since the mass density ρ is given and is constant for all y and t, then through (2.1), prescribing velocity (and thus also acceleration) at $y = 0$ and $y = L$ also prescribes the spatial derivative of shear stress, τ_y, at these points. Mathematically speaking, prescribing velocity at $y = 0$ and $y = L$ is equivalent to giving Neumann boundary conditions on the shear stress τ; the imposition of shear stress directly at the boundaries is known as a Dirichlet boundary condition on τ.

In the Dirichlet case, the prescribed shear stress at $y = L$ is taken to be positive and increasing; more precisely, we impose that

$$\tau(L,t) = D(t), \tag{2.4}$$

where the known function $D(t)$ satisfies $D(t) > 0$ and $D'(t) > 0$ for all $t > 0$. Also, $D(t)$ satisfies $D(0) = 0$, and it is taken to be continuously differentiable for all $t \geq 0$. At $y = 0$, the shear stress is imposed to be zero: $\tau(0,t) = 0$ for all $t > 0$. In the Neumann case, the prescribed spatial gradient of shear stress at $y = L$

is also taken to be positive and increasing:

$$\tau_y(L,t) = N(t), \tag{2.5}$$

where $N(t)$ is given and satisfies $N(t) > 0$ and $N'(t) > 0$ for all $t > 0$. Similarly, $N(t)$ satisfies $N(0) = 0$, and is taken to be continuously differentiable for all $t \geq 0$. At $y = 0$, the spatial gradient of the shear stress is imposed to be zero: $\tau_y(0,t) = 0$ for all $t > 0$.

In each of the Dirichlet and Neumann cases, the material is taken to be stress-free at $t = 0$:

$$\tau(y,0) = 0 \quad \text{for all } 0 \leq y \leq L. \tag{2.6}$$

Then, for $t > 0$, the shearing at $y = L$ begins, either through the prescribed shear stress, $D(t)$, in the Dirichlet case, or through the prescribed spatial gradient of the shear stress, $N(t)$, in the Neumann case. Since $D'(t) > 0$ for all $t > 0$, there exists exactly one time $t_D^* > 0$ such that $D(t_D^*) \equiv \tau(L, t_D^*) = \eta\gamma^*$: an interface point appears at $y = L$ at this time t_D^*. Before this critical time, the whole domain $(0, L)$ is hard and thus deforms according to (2.2). Differentiating (2.2) with respect to t gives

$$\tau_t = \eta u_{yt} = \eta u_{ty}, \tag{2.7}$$

since the unsoftened effective viscosity η is constant in both space and time.

Remark. *Mixed partial derivatives are applied from left to right—that is, for example*

$$u_{yt} = \frac{\partial}{\partial t}(u_y).$$

In the final equality, we assumed the velocity u was sufficiently smooth so as to allow us to swap the order of the mixed derivative. This assumption is in fact unnecessary, but a more subtle method is required to derive the same equation without invoking it—see the forthcoming paper for details.

Similarly, differentiating (2.1) with respect to y gives

$$\tau_{yy} = \rho u_{ty}, \tag{2.8}$$

since the mass density ρ is constant in both space and time. Then, rearranging each of (2.7) and (2.8) for u_{ty} and then eliminating this gives

$$\frac{1}{\eta}\tau_t = \frac{1}{\rho}\tau_{yy};$$

or equivalently

$$\tau_t = \nu\tau_{yy} \quad \text{if } \tau(y,t) < \eta\gamma^*, \tag{2.9}$$

where we have set $\nu := \eta/\rho$. Equation (2.9) describes the diffusion of local shear stress in hard regions—that is, zones where the local shear stress $\tau(y,t)$ is below the threshold value $\eta\gamma^*$. In particular, in the Dirichlet case, it applies throughout the domain $(0, L)$ for times t satisfying $0 \leq t \leq t_D^*$.

It can be shown—see the forthcoming paper for details—that, in the Neumann case, there exists a similar critical time $t_N^* > 0$ such that $\tau(L, t_N^*) = \eta\gamma^*$, and so, as with the Dirichlet case, equation (2.9) also holds throughout the domain $(0, L)$ for times t satisfying $0 \leq t \leq t_N^*$.

Remark. *Instead of differentiating* (2.2) *with respect to* t *and* (2.1) *with respect to* y*, and then solving for and eliminating* u_{ty}*, we could have simply elected to differentiate* (2.2) *with respect to* y *and then eliminated* τ_y *from the resulting equation and from* (2.1)*. This also would have produced a diffusion equation, but for* u *and not* τ*:*

$$u_t = \nu u_{yy} \quad \text{if } u_y(y,t) < \gamma^*.$$

Although simpler to derive, this diffusion equation is in fact less convenient than (2.9) *for the purposes of formulating a free boundary problem. Indeed, the condition that establishes whether this equation applies at a given spacetime point* (y,t)*—namely,* $u_y(y,t) < \gamma^*$*—involves the spatial derivative of the equation's unknown* u*; whereas the condition that establishes whether* (2.9) *applies at a given spacetime point* (y,t)*—namely,* $\tau(y,t) < \eta\gamma^*$*—involves directly the equation's unknown* τ*, making it more explicit and thus more readily implementable.*

Hence, in the Dirichlet case, the following equations apply for times t satisfying $0 < t \leq t_D^*$,

$$\tau = 0 \qquad y = 0, \tag{2.10}$$
$$\tau_t = \nu \tau_{yy} \qquad 0 < y < L, \tag{2.11}$$
$$\tau = D(t) \qquad y = L, \tag{2.12}$$

and in the Neumann case, the following equations apply for times t satisfying $0 < t \leq t_N^*$,

$$\tau_y = 0 \qquad y = 0, \tag{2.13}$$
$$\tau_t = \nu \tau_{yy} \qquad 0 < y < L, \tag{2.14}$$
$$\tau_y = N(t) \qquad y = L. \tag{2.15}$$

Both system (2.10)-(2.12) and system (2.13)-(2.15) are supplemented by the same initial condition $\tau(y, 0) = 0$ for y satisfying $0 \leq y \leq L$.

After the critical times t_D^* and t_N^*, since $D'(t) > 0$ and $N'(t) > 0$ for all $t > 0$, there will be points in the domain experiencing shear stress values exceeding $\eta\gamma^*$, as well as other points still experiencing a shear stress below this threshold. These regions will be separated by interface points at which the shear stress exactly equals $\eta\gamma^*$. Moreover, since $D'(t) > 0$ and $N'(t) > 0$ for all $t > 0$, $\tau(L, t) \neq \eta\gamma^*$ for any $t > t_D^*$ (or for any $t > t_N^*$ in the Neumann case), and so there will only ever be one interface point, separating a hard region from a shear band above it. Labelling by $y = s(t)$ the time-dependent position of this unique interface point, the field equations describing the free boundary problem are

$$\tau = 0 \text{ or } \tau_y = 0 \qquad y = 0, \tag{2.16}$$
$$\tau_t = \nu \tau_{yy} \qquad 0 < y < s(t), \tag{2.17}$$
$$\tau = \eta\gamma^* \qquad y = s(t), \tag{2.18}$$
$$[\tau_y] = 0 \qquad y = s(t), \tag{2.19}$$
$$\tau_t = \delta\nu \tau_{yy} \qquad s(t) < y < L, \tag{2.20}$$
$$\tau = D(t) \text{ or } \tau_y = N(t) \qquad y = L, \tag{2.21}$$

where equations (2.16)-(2.21) hold for $t > t_D^*$ in the Dirichlet case, or $t > t_N^*$ in the Neumann case. The diffusion equation (2.20) describing the evolution of shear stress in the shear band is derived as equation (2.17) was, but by differentiating (2.3) and not (2.2) with respect to t, as $u_y > \gamma^*$ in shear bands, by definition. For the purposes of this differentiation with respect to t, we recall that δ and γ^* are both taken to be constant in space and time.

Equation (2.18) is again the condition that characterises an interface point. Since the diffusion equations in both the hard region and the shear band involve second derivatives in space y, a second condition on the shear stress is needed to track the interface point. This is provided by (2.19), which ensures that there is no slip at interface points and that linear momentum is locally conserved at interface points (see the forthcoming paper for details of the derivation of this condition). The expression $[\tau_y]$ denotes the jump in τ_y across $y = s(t)$ at a given time $t > 0$, and is defined as

$$[\tau_y] \equiv \lim_{y \to s(t)^+} \tau_y(y, t) - \lim_{y \to s(t)^-} \tau_y(y, t),$$

where $y \to s(t)^+$ stands for "y approaching $s(t)$ from above", and $y \to s(t)^-$ for "y approaching $s(t)$ from below". In words, the jump $[\tau_y]$ gives the signed size of the discontinuity in τ_y at the point $y = s(t)$, at a given time $t > 0$. In particular, (2.19) states that the jump in the spatial gradient of shear stress, τ_y, must always be zero at an interface point—that is, in order to conserve linear momentum at an interface point, τ_y must always be continuous at $y = s(t)$.

For system (2.16)-(2.21) to be well-posed, it needs to supplemented by initial data at $t = t_D^*$ in the Dirichlet case, or at $t = t_N^*$ in the Neumann case. In the Dirichlet case, we give this in the form of the

function $\tau_D^*(y)$, the solution of system (2.10)-(2.12), evaluated at $t = t_D^*$; and in the Neumann case, in the form of the function $\tau_N^*(y)$, the solution of system (2.13)-(2.15), evaluated at $t = t_N^*$. By standard theory of parabolic equations, these functions exist and are unique, but cannot be computed exactly. Nevertheless, their asymptotic behaviour can be determined exactly, which acts to serve the asymptotic analysis of the model, outlined in the following section.

3 Outline of Asymptotic Analysis of the Shear Band Model

The goal of the asymptotic analysis in the forthcoming paper is to determine the leading-order behaviour of the interface point's trajectory, $s(t)$, in both the Dirichlet and Neumann cases. Herein, we summarise the methods used in the paper to accomplish this.

3.1 Dirichlet case

After selecting the Dirichlet conditions in (2.16) and (2.21), general small scalings in space y, time t, and shear stress τ are introduced into equations (2.16)-(2.21). The scaled equations reveal that δ is the distinguished small scale for each of the variables y, t and τ. This scale is "distinguished" in the sense that, at this scale, all the governing equations balance so as to ensure that none degenerate to a triviality after taking the limits of small space, time, and shear stress.

In this distinguished limit, the small scalings of space y, time t and shear stress τ are

$$y = L(1 - \delta\overline{y}), \quad t = t_D^* + \frac{\delta L^2}{\nu}\overline{t}, \quad \tau = \eta\gamma^*(1 + \delta\overline{\tau}). \tag{3.1}$$

Each of the variables has also been scaled such that their overlined counterparts are dimensionless and are order 1. (For a precise definition of the latter concept, see [9], for example.) In addition, the spatial scaling enforces that, for consistency, $s(t)$ must also be scaled as $s = L(1 - \delta\overline{s})$. Also, we note that, as well as being scaled, space has been flipped, for convenience, so that the shearing is applied at $\overline{y} = 0$, and similarly that shear stress has been shifted such that $\overline{\tau} = 0$ is the threshold value, again for mathematical convenience.

Then, in the asymptotic limit $\delta \searrow 0$, the scaled equations become the following one-phase problem,

$$\overline{\tau} = \overline{t} \qquad \overline{y} = 0, \tag{3.2}$$

$$\overline{\tau}_{\overline{t}} = \overline{\tau}_{\overline{y}\overline{y}} \qquad 0 < \overline{y} < \overline{s}(\overline{t}), \tag{3.3}$$

$$\overline{\tau} = 0 \qquad \overline{y} = \overline{s}(\overline{t}), \tag{3.4}$$

$$\overline{\tau}_{\overline{y}} = -k, \qquad \overline{y} = \overline{s}(\overline{t}), \tag{3.5}$$

$$\overline{\tau}(\overline{y}, 0) = -k\overline{y}, \qquad 0 \le \overline{y} < \infty, \tag{3.6}$$

where $k \equiv \tau_y(L, t_D^*)/D'(t_D^*)$. The number $\tau_y(L, t_D^*)$ can be computed by numerically solving (2.10)-(2.12), supplemented by the stress-free initial condition ($\tau(y, 0) = 0$ for all y satisfying $0 \le y \le L$). For $\overline{t} > 0$, the shear stress in the hard region $\overline{y} > \overline{s}(\overline{t})$ linearly decreases from $\tau = \eta\gamma^*$ (which is equivalent to $\overline{\tau} = 0$ in the scaled variables) at $\overline{y} = \overline{s}(\overline{t})$—it is in this sense that system (3.2)-(3.6) is a one-phase problem: the shear stress in the hard region has taken a particularly easy form in this distinguished limit.

Applying formal asymptotic methods to system (3.2)-(3.6) with $\overline{t}$ large (see the forthcoming paper for details), the leading-order trajectory of the interface point, in terms of the original dimensional variables s and t, is given by

$$s(\hat{t}) \sim L - \sqrt{2\delta\hat{t}\ln\left(\frac{\hat{t}}{\delta L^2}\right)}\left(1 - \frac{\ln\left(\ln\left(\frac{\hat{t}}{\delta L^2}\right)\right)}{\ln\left(\frac{\hat{t}}{\delta L^2}\right)} - \frac{\ln\left(\frac{k}{2}\sqrt{\pi}\right)}{\ln\left(\frac{\hat{t}}{\delta L^2}\right)}\right), \tag{3.7}$$

where $\hat{t} \equiv \nu t - L^2 t_D^*$. This asymptotic expansion for the growth of the shear band with time involves the macroscopic height L of the sample of energetic material, the boundary datum $D(t)$, and the material-specific quantities δ and $\nu \equiv \eta/\rho$, meaning comparison against experiment can be made, for different types of energetic material. We also note that, in agreement with physical intuition, the rate of shear band growth increases with δ—this increases the rate of shear stress diffusion within the shear band—and with $D'(t_D^*)$—this increases the influx of shear stress at the critical time t_D^*. The leading-order behaviour of shear stress in both the shear band and the hard region are also computed in the forthcoming paper.

3.2 Neumann case

The formal asymptotic methods required to analyse the Neumann case are somewhat more mathematically novel and complex than those used for the Dirichlet case—full details of the techniques used are given in the forthcoming paper.

First, space y, time t and shear stress τ are non-dimensionalised and shifted as follows,

$$y = L(1-\tilde{y}), \quad t = t_N^* + \frac{L^2}{\nu}\tilde{t}, \quad \tau = \eta\gamma^*(1+\tilde{\tau}).$$

Under these scalings and shifts, equations (2.16)-(2.21) (with the Neumann boundary conditions selected) become

$$\begin{aligned}
\tilde{\tau}_{\tilde{y}} &= -N(\tilde{t}) && \tilde{y} = 0 && (3.8)\\
\tilde{\tau}_{\tilde{t}} &= \delta\tilde{\tau}_{\tilde{y}\tilde{y}} && 0 < \tilde{y} < \tilde{s}(\tilde{t}) && (3.9)\\
\tilde{\tau} &= 0 && \tilde{y} = \tilde{s}(\tilde{t}) && (3.10)\\
[\tilde{\tau}_{\tilde{y}}] &= 0 && \tilde{y} = \tilde{s}(\tilde{t}) && (3.11)\\
\tilde{\tau}_{\tilde{t}} &= \tilde{\tau}_{\tilde{y}\tilde{y}} && \tilde{s}(\tilde{t}) < \tilde{y} < 1 && (3.12)\\
\tilde{\tau}_{\tilde{y}} &= 0 && \tilde{y} = 1, && (3.13)
\end{aligned}$$

where $\tilde{s}(\tilde{t}) \equiv 1 - s(t_N^* + L^2\tilde{t}/\nu)/L$. Each of the equations applies for $\tilde{t} > 0$, and the system as a whole is supplemented by the initial data $\tau_N^*(y)$, after appropriately rescaling τ and y.

As in the Dirichlet case, general small scalings in (new) space $\tilde{y}$, (new) time $\tilde{t}$ and (new) shear stress $\tilde{\tau}$ are substituted into system (3.8)-(3.13). However, unlike in the Dirichlet case, where the distinguished limit readily presented itself, methodical matched asymptotics must be applied to the scaled equations to reveal that $\tilde{t}$ of order δ^2 is the distinguished timescale of the Neumann case. For $\tilde{t}$ very small (in particular, smaller than this distinguished timescale δ^2), the leading-order growth of the shear band with time is

$$s(t) \sim L - \frac{2h_2\nu}{N(t_N^*)L}(t - t_N^*) + \frac{16h_2^2\nu}{3N(t_N^*)\sqrt{\pi}L} \cdot \frac{(1-\delta)}{\delta}(t - t_N^*), \tag{3.14}$$

where, in analogy to k in the Dirichlet case, the number h_2 is related to the initial data τ_N^* and can be computed numerically. The forthcoming paper also determines the leading-order behaviour of shear stress in both the shear band and the hard region.

The timescale $\tilde{t}$ of order δ^2 is distinguished in the sense that the above expansion for $s(t)$ (and also those for shear stress in the shear band and in the hard region) is no longer asymptotic and so breaks down at this timescale. Thus, in order to proceed, the matched asymptotics must be reapplied at the distinguished timescale $\tilde{t}$ to produce expansions that apply at these times without breaking down. These calculations determine that, at this distinguished timescale, the leading-order growth of the shear band is given implicitly by the following integral equation,

$$s(t) \sim L - \frac{2h_2\nu}{N(t_N^*)L}(t - t_N^*) + \frac{\nu}{\delta^4 L^3\sqrt{\pi}} \int_{t_N^*}^{\frac{\nu t}{\delta^2 L^2}} \frac{s'(\xi)}{\sqrt{t-\xi}}(L - s(\xi))\,\mathrm{d}\xi, \tag{3.15}$$

which cannot be solved exactly. Nevertheless, we do note that taking t small in (3.15) recovers the first two terms in (3.14) (see the forthcoming paper for full details), indicating that no intermediary distinguished timescales lie between the very short times considered previously and the timescale $\tilde{t}$ of order δ^2, and thus that the respective expansions at these two timescales match as we transition between them. The forthcoming paper also computes the leading-order behaviour of the shear stress in both the shear band and the hard region at the distinguished timescale $\tilde{t}$ of order δ^2.

Moreover, the forthcoming paper applies further perturbation methods to times of order 1, but these cannot be summarised concisely and precisely here.

4 Conclusions

A mathematical model of shear band onset and growth is developed, using a shear-thinning rheology to decouple the mechanical and thermal problems. As in previous models by Curtis, a one-dimensional problem is obtained by the homogeneity of simple shear. However, in this work, the shear stress is solved for using the equations describing the local conservation of linear momentum and the shear-thinning rheology, along with suitable boundary conditions, and is not assumed to be known *a priori*, as in Curtis's works. Moreover, the shear-thinning rheology allows for stress states strictly larger than the threshold yield value, unlike the saturation of stress that is characteristic of perfect plasticity, and so permits ever-increasing stresses within shear bands, a critical property of shear bands in reality.

The field equations describing the evolution of shear stress after the onset of a shear band are treated in the limit of small δ, the ratio of the effective viscosity in the shear band to that in the hard region. This limit describes a material that behaves extremely plastically, and so will give rise to severe shear banding, and also facilitates the formal asymptotic methods used to analyse the model. Two sets of boundary data are considered: prescribed increasing shear stress at the sheared boundary, and prescribed increasing velocity at the sheared boundary. These constitute Dirichlet and Neumann boundary data on shear stress, respectively. In each case, a distinguished timescale is determined (time after onset of order δ in the Dirichlet case, and of order δ^2 in the Neumann case), and the leading-order growth of the shear band with time is computed at the distinguished timescale in both cases. In the Neumann case, calculation of the distinguished timescale is more subtle than in the Dirichlet case. The leading-order growth of the shear band at very short times is also computed in the Neumann case, and serves to reveal the distinguished timescale. Each of the expansions for shear band growth with time involve geometrical and rheological data, and so comparison against experiment can be made, for different types of energetic material.

In summary, the great benefits of the asymptotic analyses we have performed are that they have made explicit the estimated size of the shear band and the timescales within which it grows, for both the Dirichlet and the Neumann problem. We expect good agreement of the model with empirical results after calibration of the material parameters, as soon as such data can be obtained. Moreover, we envisage that these explicit asymptotic calculations could serve to augment a finite element numerical scheme. If huge strain rates begin to accumulate within a thin zone, indicating the onset of a shear band at that location, the scheme could make use of these analytical formulae to compute shear stress within these zones, as well as the trajectory of the boundaries of these zones, thereby preventing the large numerical inaccuracies and costs that ensue from attempting to compute these quantities directly within the finite element scheme.

References

[1] Field, J. E.; Swallowe, G. M.; Heavens, S. N. Ignition mechanisms of explosives during mechanical deformation. *Proc. R. Soc. Lond. A.* **1982**, 382(1782):231–244.

[2] Boyle, V.; Frey, R.; Blake, O. Combined pressure shear ignition of explosives. *9th Symposium (International) on Detonation.* **1989**.

[3] Chen, H. C.; Nesterenko, V. F.; LaSalvia, J. C.; Meyers, M. A. Shear-induced exothermic chemical reactions. *Le Journal de Physique IV.* **1997**, 7 (C3):C3-27.

[4] Dienes, J. K. On reactive shear bands. *Physics Letters A.* **1986**, 118(9):433-438.

[5] Frey, R.B. The initiation of explosive charges by rapid shear. Technical report, DTIC Document. 1980.

[6] Afanas'ev, G. T.; Bobolev, V. K. Initiation of solid explosives by impact. *Israel Program for Scientific Translations.* **1971**.

[7] Curtis, J. P. A Model of Explosive Ignition due to Pinch. *Proceedings of the 38th International Pyrotechnics Seminar, Denver, Colorado, USA.* **2012**, 207-216.

[8] Curtis, J. P. Explosive Ignition due to Adiabatic Shear. *Proceedings of the 39th International Pyrotechnics Seminar, Valencia, Spain.* **2013**.

[9] Murray, J. D. Asymptotic Analysis. *Applied Mathematical Sciences 48.* Springer–Verlag. **1984**.